Synthesis and characterisation properties of the Sb–SnO_2–SiO_2 composite powder with the correlation analysis of resistivity and dispersion

Jiawei Tang[1], Zong Liu[1], Chunhui Zhang[1] ✉, Xiaofei Meng[1], Suoyang Li[1], Yi Pan[1], Xiaoyu Wu[1], Zheng Yan[1], Xinghua Hao[2], Honglei Zhuang[2]

[1]*School of Chemical & Environmental Engineering, China University of Mining & Technology (Beijing), Beijing 100083, People's Republic of China*
[2]*Xizang Sinorichen Environmental Protection Corp., Ltd. Shannan, Tibet Autonomous Region 856100, People's Republic of China*
✉ *E-mail: ZCHcumtb@hotmail.com*

Published in Micro & Nano Letters; Received on 7th April 2019; Revised on 26th July 2019; Accepted on 15th August 2019

Multi-group orthogonal experiments cooperating MATLAB stimulation were employed to synthesise antimony-doped tin oxide (ATO) (Sb–SnO_2)-doped silica (ATO/SiO_2) composite powder with high conductivity and dispersivity analysis. Results suggested that the resistivity ranged from 3.9 to 300 Ω cm while the nano-silica doping amount ranged from 0 to 1.5% (mass ratio) under the best parameters of Sb-doped content of 9.5 mol%, 3 precursor wash times, calcination temperature of 750°C, gelling reaction temperature of 45°C and calcination time of 2 h. Both the ATO and ATO/SiO_2 particles were characterised by X-ray diffraction, Fourier transform infrared spectroscopy, and scanning electron microscope studies to prove that the addition of silica could not only increase the specific surface area and resistivity of particles, but also reduce the agglomeration of particles. The relationship between conductivity and dispersion of composite powder (Sb–SnO_2−SiO_2) dominated by different nano-silica content could be simulated by the 'logistic function model', which has important guiding significance for the preparation of composite powders with prominent characteristics.

1. Introduction: With the rapid development of the superconducting material technology, nanoscale conductive materials have been aroused widespread concern and exploitation over the past decades [1, 2]. Antimony-doped tin oxide (ATO, Sb–SnO_2) is considered as an important member of transparent conductive oxides due to the characteristic of infrared light insulation, good stability as well as its chemical and environmental stabilities, which are proverbially used in the fields of optoelectronics [3, 4], electrochromic devices [5], solar cells, and liquid crystal display [6]. For applications involving electricity and optics, nanoparticulate ATOs are preferred since the function of reducing the particle size is to improve the catalytic properties [7]. Different from the traditional conductive medium, ATO is the solid solution of Sb-doped SnO_2 leading to the ATO films possessing high conductivity due to that electrons can tunnel easily in either direction between the adsorbed electroactive species and the SnO_2 conduction band [8, 9]. Accordingly, the photoelectric properties of ATO nanoparticles are closely related to the Sb content [10–12]. Previous academic research reported that under the optimum parameters of Sb doped content was 11 mol%, calcination temperature of 800°C and calcination time of 0.75 h, the conductivity of ATO powder in the validation experiment could reach up to 7.65 S cm^{-1} with smaller diameter and higher transmittance [13]. Actually, the nanometer powder in the coating dispersion and stability is the key function of nanoscale composite coating preparation, and the nanometer size preparation is one of the critical factors of nano transparent heat insulation coating being prepared successfully [14].

It is well known that the load application on the composites is mainly transferred to be fillers via the interface. Therefore, for excellent properties, the addition of specific modifiers is necessary to enhance the properties of composite powders. Up to now, more research on ATO powders is focused on how to reduce the resistivity of ATO powders and agglomeration of particles to further improve their photoelectric effect [15]. Relevant literature has evidence of deposited ATO nanoparticles onto a talc matrix by co-precipitation to prepare Sb–SnO_2/talc composite conductive powders and demonstrated that the resistivity of the composite conductive powders was less than 10 Ω cm under optimum conditions [2]. The nano-silica (nano-SiO_2) due to its small particle size, high dispersion, non-toxicity and the properties of insoluble water has wide application prospects in catalysis, light absorption and magnetic medium within the new materials field [16]. It had been proved from Chen *et al.*[10] that the nano-homogeneous films prepared by ATO conductive powder doped nano-SiO_2 were uniformly dispersed, and the optical properties of the composite films are significantly improved.

Based on the above researches, in this study, the robust parameter design (RPD) method was carried out in collaboration with MATLAB simulation software to further investigate the synthesis conditions of ATO powder with high conductivity and stability by doping nano-SiO_2. The objectives of this paper are: (i) to obtain the optimum process for preparing ATO powder with the lowest resistance by chemical coprecipitation method; (ii) to explore the influence of different nano-SiO_2 addition on the resistance of ATO powders, and to characterise the difference between the two powders by X-ray diffraction (XRD), scanning electron microscope (SEM), and Fourier transform infrared spectroscopy (FT-IR); (iii) to clarify the relationship between the conductivity and dispersion of the composite powder prepared by the addition of nano-SiO_2.

2. Experimental section

2.1. Chemicals: The main materials needed for this experiment include stannous chloride dihydrate ($SnCl_2{\cdot}2H_2O$, AR, Xilong Chemical Co., Ltd, China), glycol ($C_2H_6O_2$, AR), antimonous chloride ($SbCl_3$, AR, Sinopharm Chemical Regent Co., Ltd, China), ammonia ($NH_3{\cdot}H_2O$, AR), nano-silica (SiO_2, AR) and a dispersant which was prepared from castor oil and ethyl cellulose, ethocel.

2.2. Experimental design: Previous studies [5, 14] have proved that the resistivity of the ATO powder was primarily influenced by several key factors such as Sb-doped content, washing times, reaction temperature, precursor washing times, as well as

Table 1 Resistivity parameters and levels of orthogonal experiment

Symbol	Process parameter	Level 1	Level 2	Level 3	Level 4
A	Sb-doped content, mol%	8.5	9	9.5	10
B	precursor washing times	1	2	3	4
C	reaction temperature, °C	30	40	50	60
D	calcination time (h)	1	1.5	2	2.5
E	calcination temperature (°C)	650	700	750	800

Table 2 Dispersion parameters and levels of orthogonal experiment

Symbol	Process parameter	Level 1	Level 2	Level 3
L	nano-SiO_2-doped amount, g/30 g ATO	0.15	0.3	0.45
M	ball milling speed, r/min	120	240	360
N	ball milling time, h	2	4	6
O	slurry pH	4	6	8

calcination temperature and time. Therefore, to obtain the order of influence of these factors on ATO particles preparation, the standard RPD with four different levels and five influence factors L_{16} (4^5) (Table 1) test was performed comprehensively. Besides, the dispersion and stability of the ATO powder in coatings was crucial to the performance which was affected by particle size, dispersant characteristics and the mixing ratio of the powder and dispersant [17, 18]. So, another RPD experiment L_9 (3^3) (Table 2) was carried out to investigate the suitable operation parameters on the balance between resistivity and dispersivity of the nanocomposite powders. The factors include the nano-SiO_2 doped amount, ball milling speed, ball milling time, and slurry pH.

2.3. Preparation and characterisation: The $SbCl_3$ and $SnCl_2{\cdot}2H_2O$ were dissolved and stirred in ethylene glycol at 40°C until the mixture became transparent, then the nano-SiO_2 was added to the solution and stirred in a similar manner. The ATO precursor was prepared from the hydrolysis of the solutions with the different Sn/Sb mole ratio and nano-SiO_2 dosage after adding ammonia that the pH and temperature of the agitated dispersion was maintained at 8 and 30, 40, 50, 60°C, respectively and kept stirring for 4 h until the ammonia vapourised completely; the resulting hydroxide suspension was washed with deionised water by centrifuging 1–4 times first, and then washed once with absolute ethyl ethanol. The obtained precursor was dried at 90°C for 4 h in a drying oven. Finally, the as-prepared dried ATO precipitate was calcinated in a pipe furnace at different temperatures as previously designed.

The crystal structures of the ATO and ATO/SiO_2 particles samples were analysed by XRD on a Rigaku D/max-2400 diffractometer with Cu Kα radiation (λ = 1.54056 Å), and FT-IR (Agilent Cary630). The morphology of the samples was observed on a HITACHI S-4800 SEM. What is more, the conductivity of the sample powder was characterised by using the pressed disc method, and 2 g of the powdered samples were measured into a polyester cavity with 0.2 MPa of pressure each time the silver paste was coated on the surface of both sides of the silver wire winding disc to connect after calcination. The resistivity (R) was measured by the digital multimeter every 10 min until the resistance change value was <0.3. The equation used to calculate can be specifically shown and written as

$$R = 1/n \cdot \sum_{i=1}^{n} \frac{R_i}{h} \quad (1)$$

where n is the repetition number of each experiment ($n \geq 6$), $R_i(\Omega)$ is the measured value via multimeter for different times, S (cm^2) and h (cm) are the area and thickness of the powder disc.

The dispersion performance of ATO/SiO_2 was characterised by the transmissivity of the superlayer dispersions after centrifugation via the spectrophotometer. In addition, the superlayer dispersions were proportionally mixed ATO powder, nano-SiO_2, anhydrous alcohol and dispersant (made of castor oil and ethyl cellulose ethoce), all stirred evenly, then followed by the use of an ultrasonic disperser and ball mill to ultrasonic and grinding treatment until the set time.

3. Results and discussion

3.1. Resistivity optimisation of ATO particles: The raw resistivity of the 16 trials reveals that the Sb-doped content, washing times and calcination temperature with 77.5% contribution that were the major influencing factors for the high conductive ATO powder preparation, while the reaction temperature and calcination time with 22.5% contribution showed a similar result with a previous study [19]. The minimum resistance value was 6.8 Ω cm while the above conditions were 9.5% of the Sn/Sb mole ratio, four times of precursor washing times, 40°C of precursor reaction temperature at 750°C of calcination temperature with 1 h, respectively. To determine the optimum parameters on the preparation of ATO powders, Sb doped content and washing times, reaction temperature and calcination time were simulated by using MATLAB software. According to the orthogonal experimental results above, simulated test influenced by the range of Sb doping (A: 8.5–10%) and precursor washing times (B: 1–4 times) to the ATO resistivity by setting the reaction temperature (C = 40 °C) and calcination time (D = 1.5 h) remained unchanged. Then, the reaction temperature (C: 30–60°C) and calcination time (D: 1–2.5 h) ranges on resistivity were also simulated under the optimal amount of Sb-doped content, washing times and a calcination temperature of 750°C. The results are as follows.

As shown in Fig. 1, the lowest resistivity occurring at Sb (mol%) doped content was between 9.5 and 10%, washing times were >3, calcination time was 2 h and the reaction time was between 40 and 55 °C. In the process of calcination at high temperature, the Sb atom is as an effective donor in the form of Sb^{5+} incorporated into the lattice, which caused the reduction of the resistivity. However, when the Sb-doped amount increased from 9.5 to 10 mol%, the increase in resistivity could be attributed to that excess Sb, which led to a part of the Sb^{5+} ions to be reduced to the Sb^{3+} state, which acted as acceptors so that the electrons created by Sb^{5+} were trapped by the acceptor levels, then increased the particle resistivity [14]. The gelation reaction is the most important step influenced by the reaction temperature in the preparation of powders which aim to generate $Sn(OH)_4$ and $Sb(OH)_3$ precipitation. When the reaction temperature was low, the precipitation reaction was not complete, which made the concentration of Sb ions in SnO_2 also low, then leading to the increase of resistance.

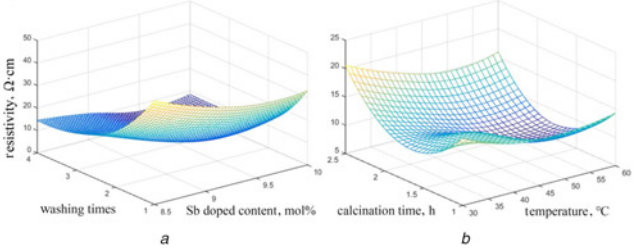

Fig. 1 *Simulation study on the ATO resistivity*
a Effect on washing times and Sb dopants
b Effect on calcination times and reaction temperature

doi: 10.1049/mnl.2019.0128

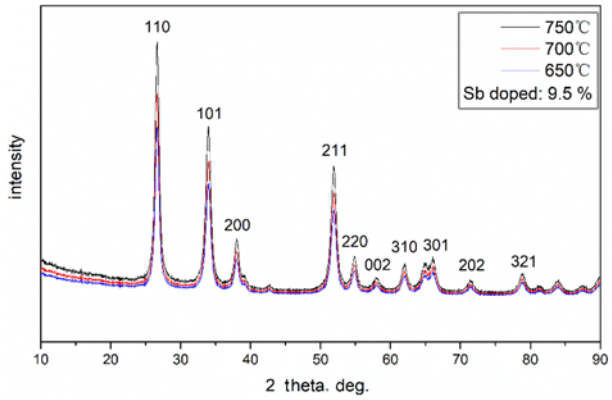

Fig. 2 *XRD patterns of ATO powder calcined at different temperatures*

So, considering the operation cost, 45°C is considered as the optimal condition.

Fig. 2 shows the XRD reflections of ATO prepared with different calcination temperatures. With the (110) reflection being the most intense, the second and third reflections were (101) and (211), which corresponded to the cassiterite structure. On increasing the calcination temperature from 650 to 750°C, diffraction peaks like (110), (101) and (211) crystal was gradually sharpened similar to a previous study [20]. Additionally, diffraction peaks of (200), (220) and (310) crystal were gradually visible, showed a trend towards integrity of the SnO_2 crystalline structure, which indicated this operation could be a suitable method to the prepared ATO. Therefore, according to the result of parameters optimisation above, multiple repetitive tests was carried out, and a lowest resistivity of 3.9 Ω cm was obtained under the optimum conditions of the Sb-doped content was 9.5 mol%, after washing three times at a gelling reaction temperature of 45°C and a calcination time of 2 h under 750°C of calcination temperature.

3.2. Dispersion optimisation of ATO/SiO_2 particles: The contribution percentage and significance degree of each factor can be obtained by analysis of variance, which will give the relative effect of the different factors on experimental responses more clearly. As tested from Table 2, the best combinations were L3 (0.45 g), M3 (360 r/min), N2 (4 h) and O1 (pH 4) which could predict that the more amount of silica added and better the grinding of the composite powders. The main factor affecting the stability of the ATO slurry being the nano-SiO_2 doping amount, followed by ball milling time, speed and slurry pH, indicated that the product slurry has higher transmissivity by adding nano-SiO_2 before the formation of the ATO precursor. Furthermore, the ball milling time exhibits more importance to slurry stability than grinding speed and slurry pH, and this can be attributed to the surface energy of powders that would be weakened in the process of ball milling, then forming space steric resistance between the dispersants and granules to increase the dispersion performance of the slurry. Fig. 3 also illustrated that the high nano-SiO_2 doped amount, and long grinding time within low pH could introduce a more stable slurry. According to the DLVO theory, the larger the zeta potential (absolute value), the higher the charge density on the surface of the particlesand the larger the electrostatic repulsion of the double layer on the particle surface. Thus, it could be deduced that the zeta potential on the surface of composite powders was increased after the dosage of nano-SiO_2. However, as the amount of SiO_2 increases, the resistance of the powder increases sharply which up to 300 Ω·cm after doping with 0.45 g of nano-SiO_2 under the optimum operating conditions.

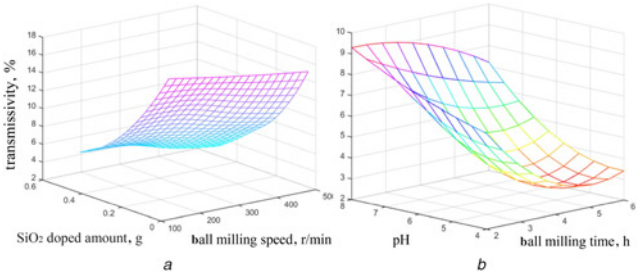

Fig. 3 *Simulation study on the ATO/SiO_2 transmissivity*
a Effect on different ball milling speed and time
b Effect on nano-SiO_2-doped amount and pH (b)

3.3. Characterisation of ATO and ATO/SiO_2 particles: The XRD result of ATO doped nano-SiO_2 (0.7 mass%) under the best optimum conditions is depicted, and in the asynthesised particles, the XRD patterns varied slightly due to the less nano-SiO_2 dose. The XRD patterns dominated the SnO_2 tetrahedral structure (square closed symbol) similar to early experiments (Fig. 2). For further investigation of the phase composition of the ATO/SiO_2 particles, Fig. 4 presents the FT-IR spectrum of (i) ATO/SiO_2 and (ii) ATO particles. As is shown that the peak near the wavenumber of 630 cm^{-1} was categorised to the stretching vibration peak of the Sn−O bond, indicated that the product from ATO and ATO/SiO_2 particles was completely crystallised. The characteristic absorption peaks of H_2O and OH appeared at 3440 cm^{-1}, 1640 cm^{-1} and 1400 cm^{-1} in both samples, suggesting that there were traces of H_2O and -OH on the surface of the sample. Compared to the IR spectrum of the ATO sample, there were some different characteristic peaks appearing at the wavenumbers 450 cm^{-1} and 1110 cm^{-1}, which could be identified as the vibration characteristic peak of Si−O after comparison with the standard card. Therefore, the FT-IR spectrum further confirmed the composition of the powder on the results of XRD.

The ATO nanoparticles were obtained by the thermal decomposition of precursor particles after calcination at 750°C.

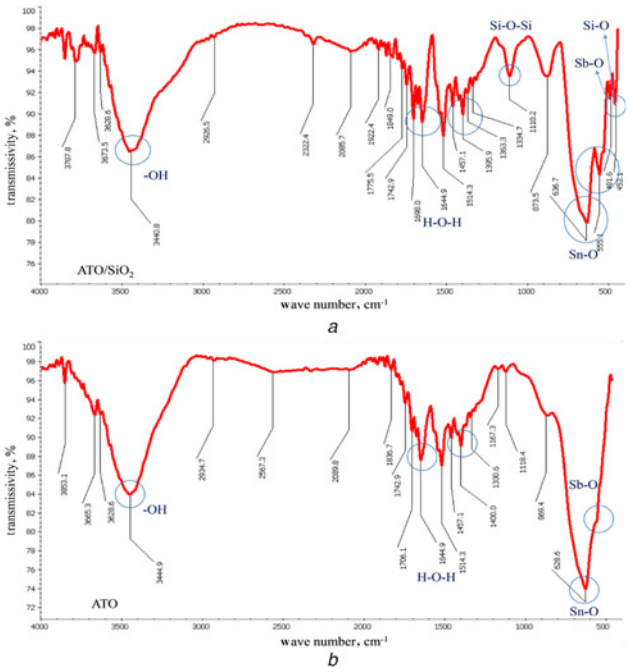

Fig. 4 *FT-IR spectrum of*
a ATO/SiO_2 particles
b ATO particles

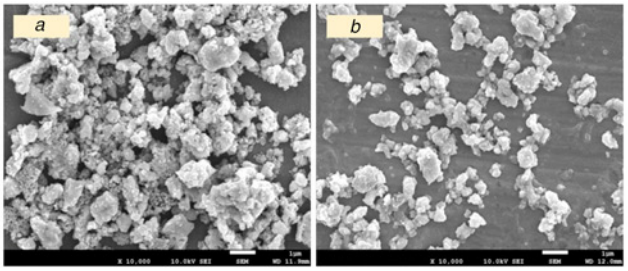

Fig. 5 *SEM image of*
a ATO particles
b ATO/SiO_2 particles

Table 3 Surface properties of ATO and ATO/SiO_2 nanoparticles

Item	Unit	ATO	ATO/SiO_2
BET surface area	m^2/g	25.0253	30.2792
Langmuir surface area	m^2/g	29.8353	35.0499
pore volume (BJH adsorption cumulative volume)	cm^3/g	0.14581	0.11873
pore size (4 V/A by BET)	nm	9.1928	9.7949
nanoparticle size	nm	239.76	198.1556

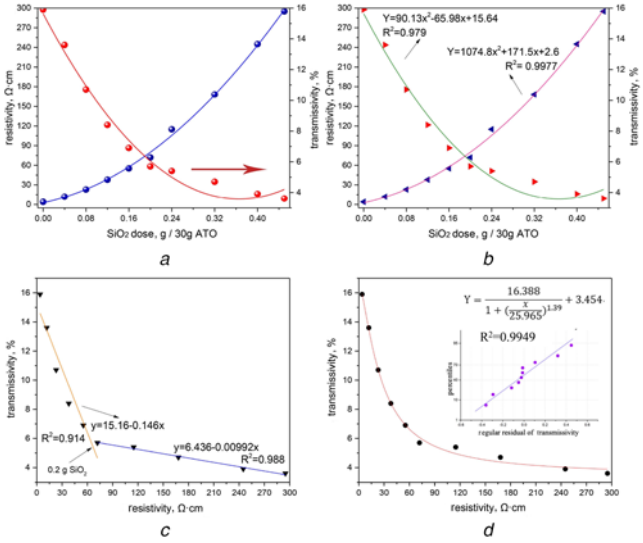

Fig. 6 *Effect of nano-SiO_2 dosage on dispersion and resistivity, and their relationships*
a Effect of SiO_2 dose on resistivity and dispersion
b Non-linear fitting for the effect of SiO_2 dose on resistivity and dispersion
c Linear fitting for the effect of ATO resistivity on dispersion
d Non-linear fitting for the effect of ATO resistivity on dispersion

The morphology of the two products was examined by SEM analysis as follows (Fig. 5). The average diameter of ATO and ATO/SiO_2 particles was evaluated to be ~0.6–1.5 μm and 0.5 μm, respectively, and severe powder agglomeration had occurred.

Agglomeration of powders is a natural phenomenon due to the nanoparticles' surface forces such as the van der Waals forces, capillary forces and electrostatic forces, which can overcome only against the gravitational and inertial forces for particles in this size range [20, 21]. Although the agglomeration of ATO was reduced after doped SiO_2, the particle size of the ATO powder was still relatively large from the microscopic morphology. Thus, the surface area, pore size and nanoparticles size were accurately measured (Table 3). Following the SEM results, ATO-doped SiO_2 particles had a bigger BET surface area (30.2792 m2/g), and pore size (9.7949 nm) within a smaller pore volume (0.1187 cm^3/g) and nanoparticles size (198 nm) than ATO, which demonstrated that the addition of silica could increase the specific surface area of ATO particles as well as the inhibitory effect on the agglomeration of powders.

3.4. Effect of SiO_2 dose on ATO resistivity and dispersivity: The above experiment suggests that with the increase of the nano-SiO_2-doped amount, the resistance of the powder increases correspondingly. The conductivity and dispersibility of the ATO powder directly affect powder utilisation leading to its significance in finding the relationship between the SiO_2 doping amount and the change in resistance. The resistivity and transmissivity change with different nano-SiO_2 dose are summarised as the following figures.

Fig. 6*a* depicts the effect of nano-SiO_2 dosage on dispersion and resistivity. While the nano-SiO_2-doped amount ranged from 0 to 0.16 g, the slurry transmissivity decreases dramatically, whereas the resistance increases slightly (0–58 Ω·cm), but the powder resistivity increases markedly after the doped amount of SiO_2 exceeded 0.67% (mass ratio). For further investigation of the corresponding changes in powder resistance and powder stability, the nonlinear fitting model was applied and showed in Fig. 6*b*, the high correlation coefficients of 0.979 and 0.9977 were attained by the quadratic equation that could be used to predicate the influence of resistivity and transmittance on the change of various nano-SiO_2 doping amounts. In addition, the correlation between resistivity and dispersion was also analysed via linear and nonlinear fitting models. Similar to earlier studies above, although accurate correlation ($R^2 = 0.914$, 0.988) could be obtained while the SiO_2 doping amount was around 0.2 g (Fig. 6*c*), a lack of consistency leads to the need for a non-linear fitting equation for accurate prediction. Thus, the non-linear logistic function model was carried out to simulate the relationship between slurry transmittance (powder dispersion) and powder resistivity (Fig. 6*d*). With the increase in the nano-SiO_2 doping amount and its resistivity, the Sb–SnO_2–SiO_2 (ATO/SiO_2) composite slurry transmissivity was reduced drastically that exhibited an 'S-type' change relationship as summarized in (2). High relevance and residual analysis can guarantee the accuracy of this equation in predicting the functional relationship between the dispersion and stability of the powders

$$Y = \frac{16.388}{1 + \left(x/25.965\right)^{1.39}} + 3.454 \tag{2}$$

4. Conclusion: The ATO and ATO-doped nano-silica (Sb–SnO_2–SiO_2) particles were obtained by co-precipitation reaction in glycol solution of tin (II) chloride pentahydrate and antimony (III) chloride. The influence of the processing parameters on the formation of low resistivity and high dispersivity ATO powder was optimised by employing RPD and MATLAB simulation. Results indicated that the main effect factors on the conductivity of ATO powder were Sb-doped content (9.5 mol%), then by precursor wash times (3), calcination temperature (750°C), gelling reaction temperature (45°C) and calcination time (2 h). The Sb–SnO_2–SiO_2 slurry dispersion experiment showed that more silica doping and longer slurry grinding time could make the slurry more stable at a low pH of 4, which catered to the characterisation results from FT-IR, BETs, and SEM that nano-SnO_2 addition could not only slow the agglomeration of ATO powder, but also increase the specific surface area and reduce the particle size. Importantly, the role of different SiO_2 doses on ATO resistivity and dispersivity was determined by linear and non-linear model fitting. As a result, the ATO/SiO_2

doi: 10.1049/mnl.2019.0128

slurry dispersibility and powder resistivity could be fitted and predicted by logistic function with high R^2 of 0.9949.

5. Acknowledgments: This work was supported by the Major Science and Technology Program for Water Pollution Control and Treatment (grant no. 2017ZX07402001), the National Key Research and Development Program of China (grant no. 2018YFC0406400) and the Special Funds for Fundamental Scientific Research Business Expenses of Central Universities (China, grant no. 2011QH01).

6 References

[1] Dai Z., Li Z., Li L, *ET AL.*: 'Synthesis and thermal properties of antimony doped tin oxide/waterborne polyurethane nanocomposite films as heat insulating materials', *Polym. Adv. Technol.*, 2011, **22**, pp. 1905–1911

[2] Wang L., Wada H., Allard L.F.: 'Synthesis and characterization of Sic whiskers', *J. Mater. Res.*, 2016, **7**, pp. 51–52

[3] Zhou S.X., Wu L.M., Shen W. D., *ET AL.*: 'Study on the morphology and tribological properties of acrylic based polyurethane/fumed silica composite coatings', *J. Mater. Sci.*, 2004, **39**, pp. 1593–1600

[4] Han H., Mayer J.W., Alford T.L.: 'Band gap shift in the indium-tin-oxide films on polyethylene napthalate after thermal annealing in air', *J. Appl. Phys.*, 2006, **100**, pp. 75–83

[5] Nooshinfar E., Bashash D., Safaroghli-Azar A., *ET AL.*: 'Melatonin promotes ato-induced apoptosis in mcf-7 cells: proposing novel therapeutic potential for breast cancer', *Biomed. Pharmacother.*, 2016, **83**, pp. 456–465

[6] Kim D.W., Kim D.S., Kim Y.G., *ET AL.*: 'Preparation of hard agglomerates free and weakly agglomerated antimony doped tin oxide (ATO) nanoparticles by coprecipitation reaction in methanol reaction medium', *Mater. Chem. Phys.*, 2006, **97**, pp. 452–457

[7] Zhang J., Gao L.: 'Synthesis and characterization of antimony-doped tin oxide (ATO) nanoparticles by a new hydrothermal method', *Mater. Chem. Phys.*, 2004, **87**, pp. 10–13

[8] Hu P. W., Yang H.: 'Controlled coating of antimony-doped tin oxide nanoparticles on kaolinite particles', *Appl. Clay Sci.*, 2010, **48**, pp. 368–374

[9] Li T., Duan J., Yang C., *ET AL.*: 'Synthesis, microstructure and magnetic properties of Heusler CO_2FeSn nanoparticles', *Micro Nano Lett.*, 2013, **8**, pp. 143–146

[10] Chen X.C.: Synthesis and characterization of ATO/siO_2 nanocomposite coating obtained by Sol–gel method. *Mater. Lett.*, 2005, **59**, pp. 1239–1242

[11] Zhang J., Wang L., Zhang Q.: 'Influence of Sb content on electromagnetic properties of ATO/ferrite composites synthesized by co-precipitation method', *J. Magn. Magn. Mater.*, 2005, **390**, pp. 107–113

[12] Zhang J., Wang L. X., Liang M. P., *ET AL.*: 'Effects of Sb content on structure and laser reflection performance of ATO nanomaterials', *T Nonferr. Metal. Soc.*, 2014, **24**, pp. 131–135

[13] Lu H. F., Hong R. Y., Wang L. S., *ET AL.*: 'Preparation of ATO nanorods and electrical resistivity analysis', *Mater. Lett.*, 2012, **68**, pp. 237–239

[14] An Q., Bai G. H., Yang Y., *ET AL.*: 'Preparation optimization of ATO particles by robust parameter design', *Mat. Sci. Semicon. Proc.*, 2016, **42**, pp. 354–358

[15] Su W. W., Wang W., Li Y. L., *ET AL.*: 'Fabrication of antimony-doped tin oxide/carbon black composite with oxygen plasma treatment for lithium-air batteries', *Mater. Lett.*, 2016, **180**, pp. 203–206

[16] Qiao B., Liang Y., Wang T. J., *ET AL.*: 'Surface modification to produce hydrophobic nano-silica particles using sodium dodecyl sulfate as a modifier', *Appl. Surf. Sci.*, 2016, **364**, pp. 103–109

[17] Rechberger F., Städler R., Tervoort E., *ET AL.*: 'Strategies to improve the electrical conductivity of nanoparticle-based antimony-doped tin oxide aerogels', *J. Sol-Gel Sci. Techn.*, 2016, **80**, pp. 660–666

[18] Luo S.X., Song Z., Li J. L.: 'Research on the dispersion uniformity and stability of nano-ATO', *J. Funct. Mater.*, 2013, **11**, pp. 1603–1606

[19] Yu S., Zheng H., Li L., *ET AL.*: 'Highly conducting and transparent antimony doped tin oxide thin films: the role of sputtering power density', *Ceram. Int.*, 2017, **43**, pp. 5654–5660

[20] Wang L.S., Lu H.F., Hong R.Y., *ET AL.*: 'Synthesis and electrical resistivity analysis of ATO-coated talc', *Powder Technol.*, 2012, **224**, pp. 124–128

[21] Chao Z., Hui Y., Guo X. Z.: 'Preparation of antimony doped tine oxide heat-insulating slurry via surface modification by vinyl triethoxy silane', *J. Ceram. Soc.*, 2014, **42**, pp. 17–21